8.2 ENVIRONMENTAL EVOLUTION OF LONG-LIVED SUPERCELLS

Casey E. Davenport*
University of North Carolina at Charlotte

1. INTRODUCTION

Long-lived supercells, defined as thunderstorms with a persistent rotating updraft for at least four hours (Bunkers et al. 2006a), can present significant hazards to the public over an extended period. For example, when comparing long-lived to short-lived supercells (lifetimes $\leq$ 2 hours), over four times as many strong tornadoes (F2 and greater) were associated with long-lived supercells; severe hail and wind gusts were also much more prevalent in long-lived events (Bunkers et al. 2006a).

The broad synoptic and mesoscale environments in which long-lived supercells form in, as well as their climatological characteristics, have been clearly elucidated by Bunkers et al. (2006a, b). Indeed, the conceptual model of where long-lived supercells tend to be observed and guidelines of environmental characteristics (Fig. 1) serves as a helpful baseline for forecasters. However, the extent to which these environmental characteristics vary over the lifetime of supercells has yet to be quantified.

The degree of environmental variability present is an important aspect that needs to be considered. It is well-understood that spatial and temporal variability is present in convective storm environments, and often influences storm intensity, longevity, and severe weather production. For example, Klees et al. (2016) documented a case from VORTEX2 wherein a tornadic supercell was in immediate proximity of a non-tornadic supercell. Notably, there were significant temporal and spatial variations in the kinematic and thermodynamic environment, with conditions more supportive of tornadoes near the tornadic storm. Davenport and Parker (2015a, b) and Gropp and Davenport (2018) have also demonstrated that shifts in the near-storm environment can lead to varying outcomes in the morphology and longevity of supercell thunderstorms.

Despite the key role of environmental variability in supercell evolution, the extent of such changes in the near-storm environment has yet to be quantified for a large sample of storms. Thus, the goal of this study is to measure thermodynamic and kinematic changes in the near-storm environment over the lifetime of long-lived supercells using a Lagrangian framework. More broadly, this effort will aid in better understanding how supercells respond to changes in their environment, and how such shifts impact their internal dynamical processes, intensity, longevity, and proclivity to produce severe weather.

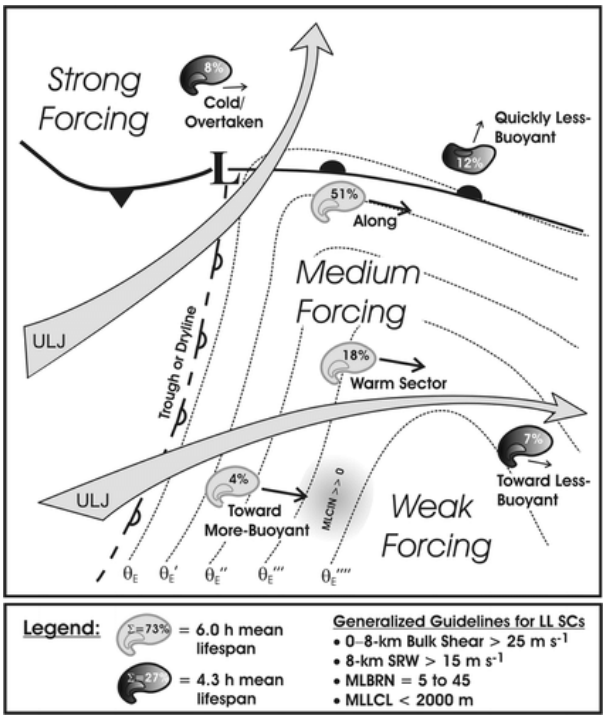

Figure 1: A conceptual model of midlatitude cyclone locations and associated long-lived supercell frequency. Guideline values for environments supportive of producing long-lived supercells are also shown. Taken from Bunkers et al. (2006b).

2. METHODS

The first step involves identifying a large number of observed long-lived supercells. The process was similar to that outlined in Bunkers et al. (2006a), which involves a manual examination of radar reflectivity data to identify long-lived storms with supercellular characteristics. This examination occurred for events within the Great Plains region between 2002 and 2017, with a focus on relatively isolated convection (e.g., Fig. 2). The geographical and storm type constraints were imposed to remove the potentially complicating factors of complex terrain and storm interactions, thus allowing for more direct connections to be made between changes in the environment and changes in storm characteristics. Each individual supercell was counted

* *Corresponding author address*: Casey E. Davenport, University of North Carolina at Charlotte, Department of Geography and Earth Sciences, Charlotte, NC 28223; email: Casey.Davenport@uncc.edu

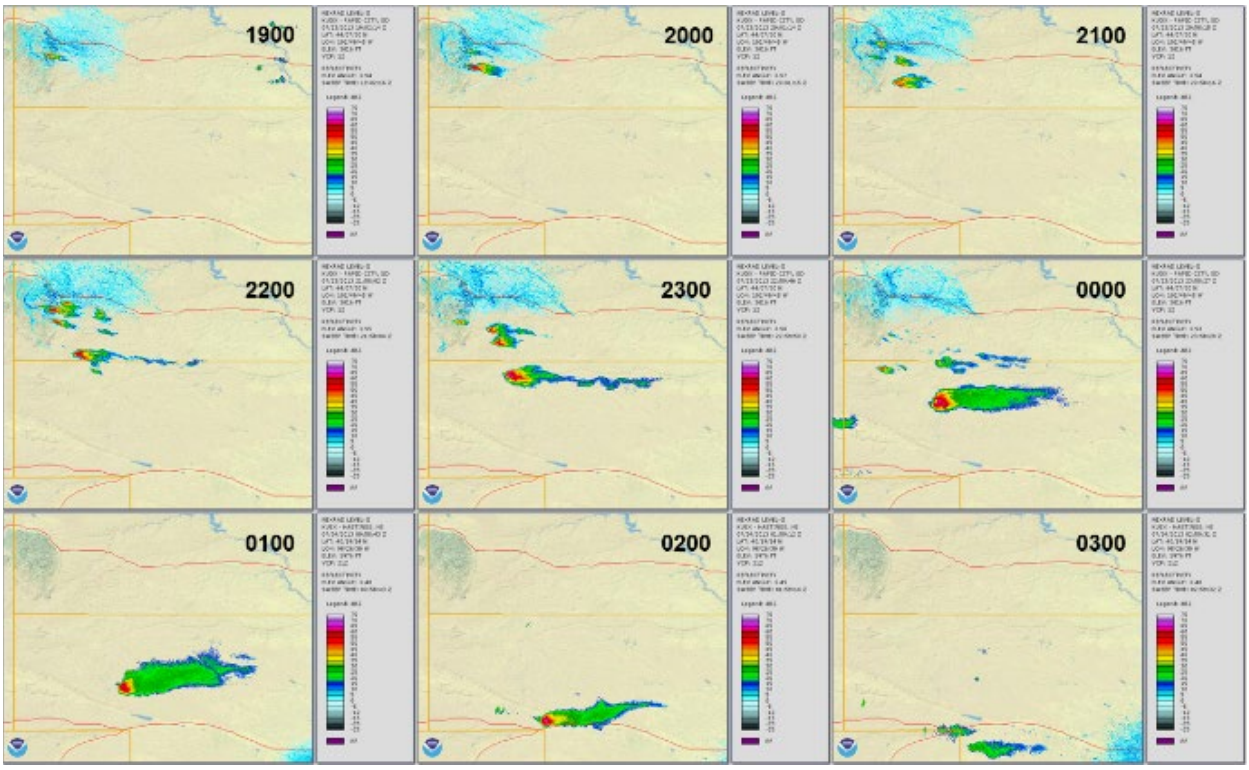

Figure 2: Radar evolution of sample long-lived supercell case from 23-24 July 2013. Times are listed in UTC.

as its own case; a total of 144 cases with available environmental data and confirmed long-lived mesocyclones were identified in this dataset.

Next, each supercell was tracked over its lifetime, with a near-storm sounding collected at each hour between initiation and dissipation of the storm. These environmental profiles were gathered from either the RUC or RAP model analysis, as available. Each sounding was manually examined to ensure representativeness and no convective contamination. A series of sample soundings for the case shown in Fig. 2 is provided in Fig. 3. From these soundings, a series of common forecasting parameters, such as convective available potential energy (CAPE), convective inhibition (CIN), bulk wind shear over a variety of layers, and storm-relative helicity (SRH), were calculated.

3. RESULTS

The climatological characteristics of this dataset, while independent from the Bunkers et al. (2006a, b) study, are very much consistent with that prior study of long-lived supercells. For example, the seasonal variability and diurnal frequency of the present dataset is quite similar; there is a peak in long-lived supercell activity in the late spring and early summer months (Fig. 4a), along with a diurnal peak near 0100 UTC (Fig. 4b). Indeed, this diurnal peak is quite prevalent in other aspects of the dataset. Notably, long-lived supercell cases are most frequently initiated in the late afternoon hours and then dissipate in the early evening hours (Fig. 5a). This is in line with the overall average supercell lifetime of 5.4 hours, nearly identical to the Bunkers et al. (2006a) value of 5.5 hours. Accordingly, the majority of cases exhibited lifetimes that were marginally long-lived (i.e., between 4-5 hours), with an exponential decrease for lifetimes longer than 5 hours (Fig. 5b).

To further emphasize the prevalence of the diurnal signal, the hourly distribution of a few select parameters will be shown. For each hour that environmental data was collected, a violin plot will be used to display the distribution of parameter values. A violin plot is similar to a box plot, but shows the full distribution of values based on the kernel density estimation; where the plot is wide (narrow), there is a greater (smaller) probability that the raw data contains that value. For completeness, the median and interquartile range of the data are also shown.

The diurnal signal is quite clear in parameters near the surface. Surface-based CAPE (CIN) is maximized (minimized) in the late afternoon hours (Fig. 6a, b) near the time of most frequent storm initiation (Fig. 5a). Instability then decreases (and inhibition increases) as

the surface cools and stabilizes near 0000 UTC. The impact of the nocturnal transition is further highlighted in the evolution of 0-1 km bulk shear, where shear significantly strengthens after 0000 UTC, in accordance with the development of the Great Plains low-level jet (Fig. 6c).

While the impact of daytime heating and cooling is clearly an important component in determining parameter values, the goal of this study is to assess how the near-storm environment evolves over the lifetime of a long-lived supercell with respect to characteristics such as storm maturity. Thus, three soundings were chosen for each case, representing the initial, mature, and dissipation stages of the storm.

Trends in environmental parameters with respect to storm maturity are generally consistent with expectations of what would/would not be supportive of deep convection, combined with the influence of the diurnal cycle. For example, instability (both surface-based and elevated) tends to weaken over time, with lowest values at the dissipation stage, while inhibition increases in magnitude (Fig. 7); both tend to be a function of daytime heating and cooling. Notably, at the dissipation stage, there tends to be sufficient MUCAPE and minimal MUCIN to sustain convection. Even so, the smaller SBCAPE and larger SBCIN values suggest that the supercells were unable to be further sustained as elevated storms.

The evolution in deep-layer bulk shear is comparatively more subtle. Even so, it is evident that there is a slight overall drop in both 0-8 and 0-6 km shear over time. The trend is more apparent in the 0-8 km layer, where both the median and the upper-most extreme values shrink by a few m/s between the initial and dissipation stages. Only slight shifts in the median are evident in the 0-6 km layer (Fig. 8).

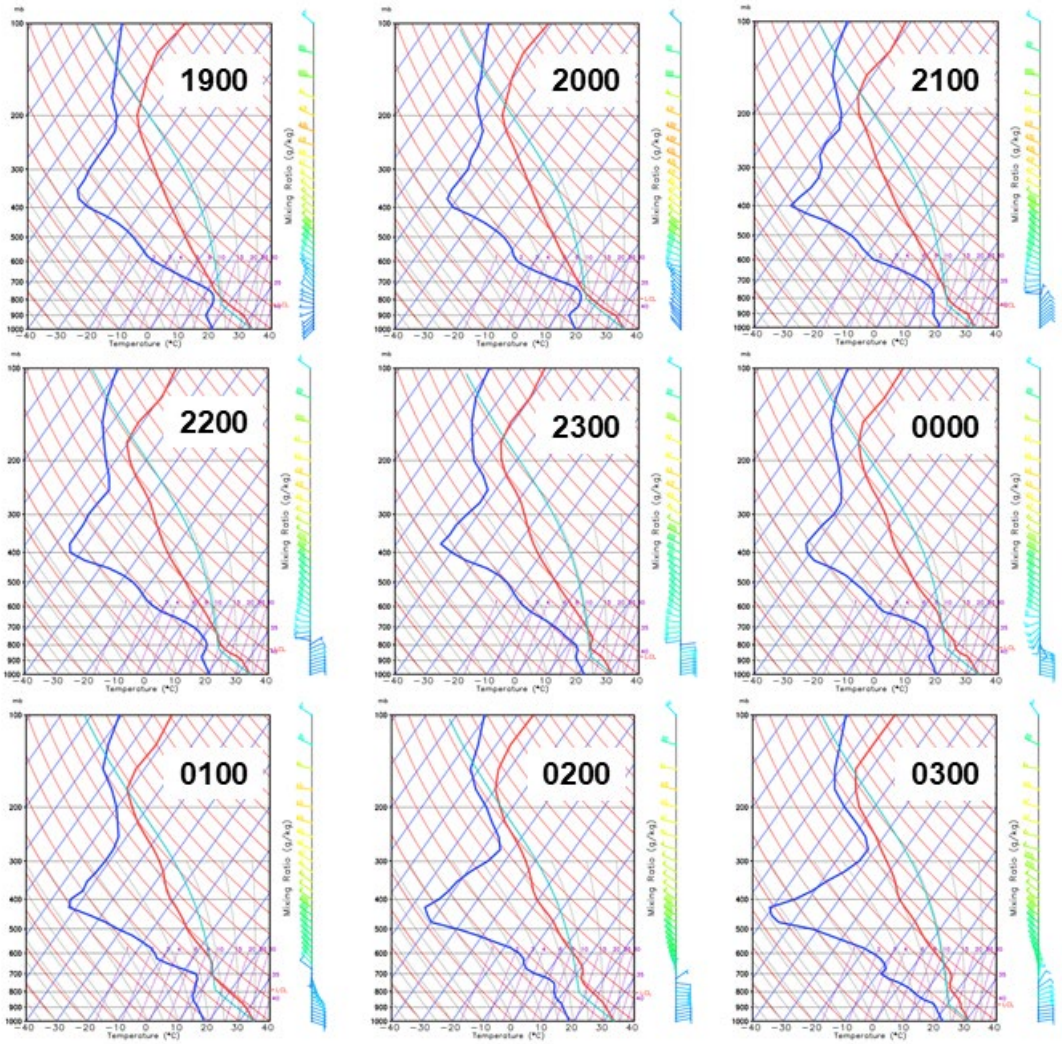

Figure 3: Near-storm model skew-T log-p soundings over the course of the lifetime of the sample supercell shown in Fig. 3.

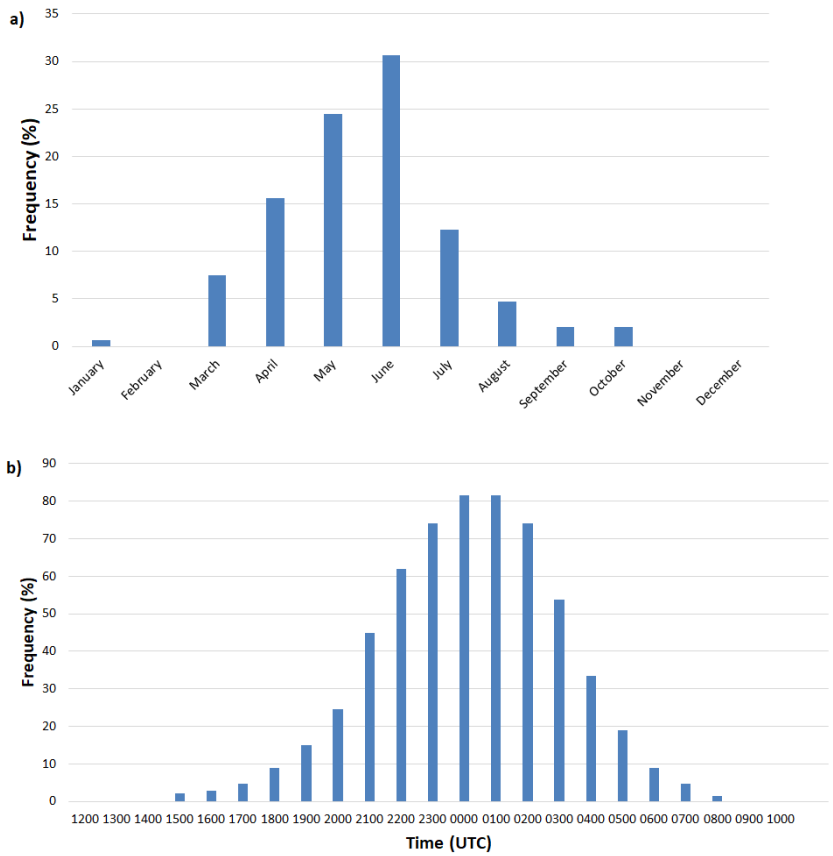

Figure 4: a) Monthly and b) hourly frequencies of occurrence of long-lived supercells.

In the low-levels, there is a marked difference in the evolution of shear in the 0-3 versus 0-1 km layers. 0-3 km shear peaks slightly at the mature stage, while 0-1 km shear notably increases over the lifetime of a long-lived supercell (Fig. 8). The latter trend is likely tied to the strong diurnal nature of supercell dissipation (Fig. 5b), where low-level shear increases following the nocturnal transition as a result of the development of the low-level jet (Fig. 6b). Accordingly, low-level SRH also tends to strongly increase as supercells mature and dissipate (Fig. 8).

4. SUMMARY AND FUTURE WORK

Thus far, it is quite clear that the pattern of daytime heating and cooling plays a strong role in regulating long-lived supercell development and dissipation, along with the characteristics of its near-storm environment. This is perhaps not too surprising given the extended longevity and typical initiation time of these storms. Accordingly, over the lifetime of a long-lived supercell, instability tends to decrease while inhibition increases. A strong diurnal signal was also evident in low-level shear and SRH, particularly in the 0-1 km layer.

Outside of the diurnal cycle, it was also apparent that deep-layer shear weakened slightly over time, perhaps as a result of a supercell "outrunning" its synoptic-scale support, though this would need to be confirmed with additional data.

This study is still in its early stages, with much work yet to be completed. Additional environmental parameters will be gathered, such as effective-layer shear and SRH. Being able to correlate environmental changes with supercell characteristics (e.g., mesocyclone strength and depth) and severe weather production is also desirable. Various subsets of this data will also be examined and compared, including very long-lived versus marginally long-lived supercells, as well as those that dissipate before versus after sunset.

5. REFERENCES

Bunkers, M.J., M.R. Hjelmfelt, and P.L. Smith, 2006a: An observational examination of long-lived supercells. Part I: Characteristics, evolution, and demise. *Wea. Forecasting*, **21**, 673—688.

Bunkers, M.J. J.S. Johnson, L.J. Czepyha, J.M. Grzywacz, B.A. Klimowski, and M.R. Hjelmfelt, 2006b: An observational examination of long-lived supercells. Part II: Environmental conditions and forecasting. *Wea. Forecasting*, **21**, 689—714.

Davenport, C.E., and M.D. Parker, 2015a: Observations of the 9 June 2009 dissipating supercell from VORTEX2. *Wea. Forecasting*, **30**, 368—388.

Davenport, C.E., and M.D. Parker, 2015b: Impact of environmental heterogeneity on the dynamics of a dissipating supercell thunderstorm. *Mon. Wea. Rev.*, **143**, 4244—4277.

Gropp, M.E., and C.E. Davenport, 2018: The impact of the nocturnal transition on the lifetime and evolution of supercell thunderstorms in the Great Plains. *Wea. Forecasting*, **33**, 1045—1061.

Klees, A.M., Y.P. Richardson, P.M. Markowski, C. Weiss, J.M. Wurman, and K.K. Kosiba, 2016: Comparison of the tornadic and nontornadic supercells intercepted by VORTEX2 on 10 June 2010. *Mon. Wea. Rev.*, **144**, 3201—3231.

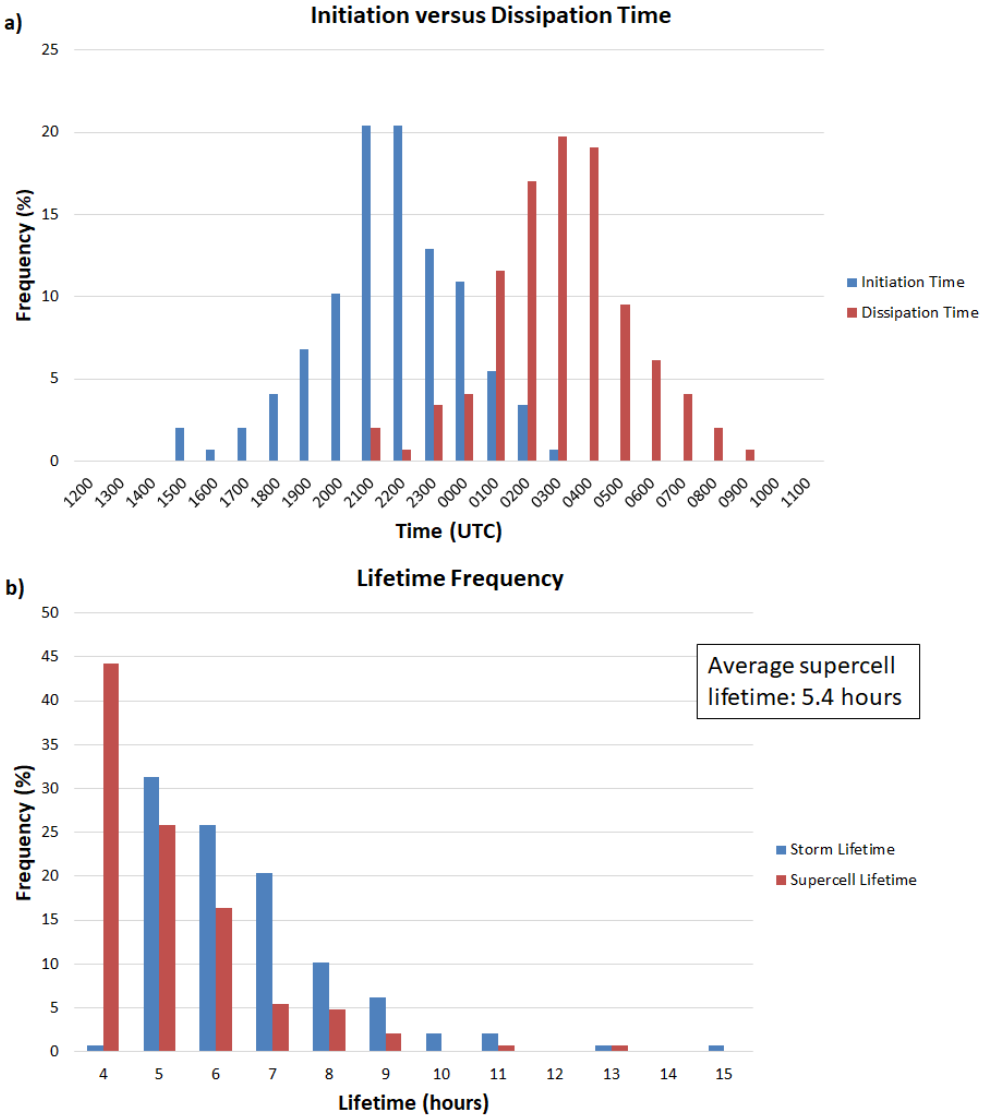

Figure 5: Frequencies of a) times of supercell initiation and dissipation and b) supercell and storm longevity.

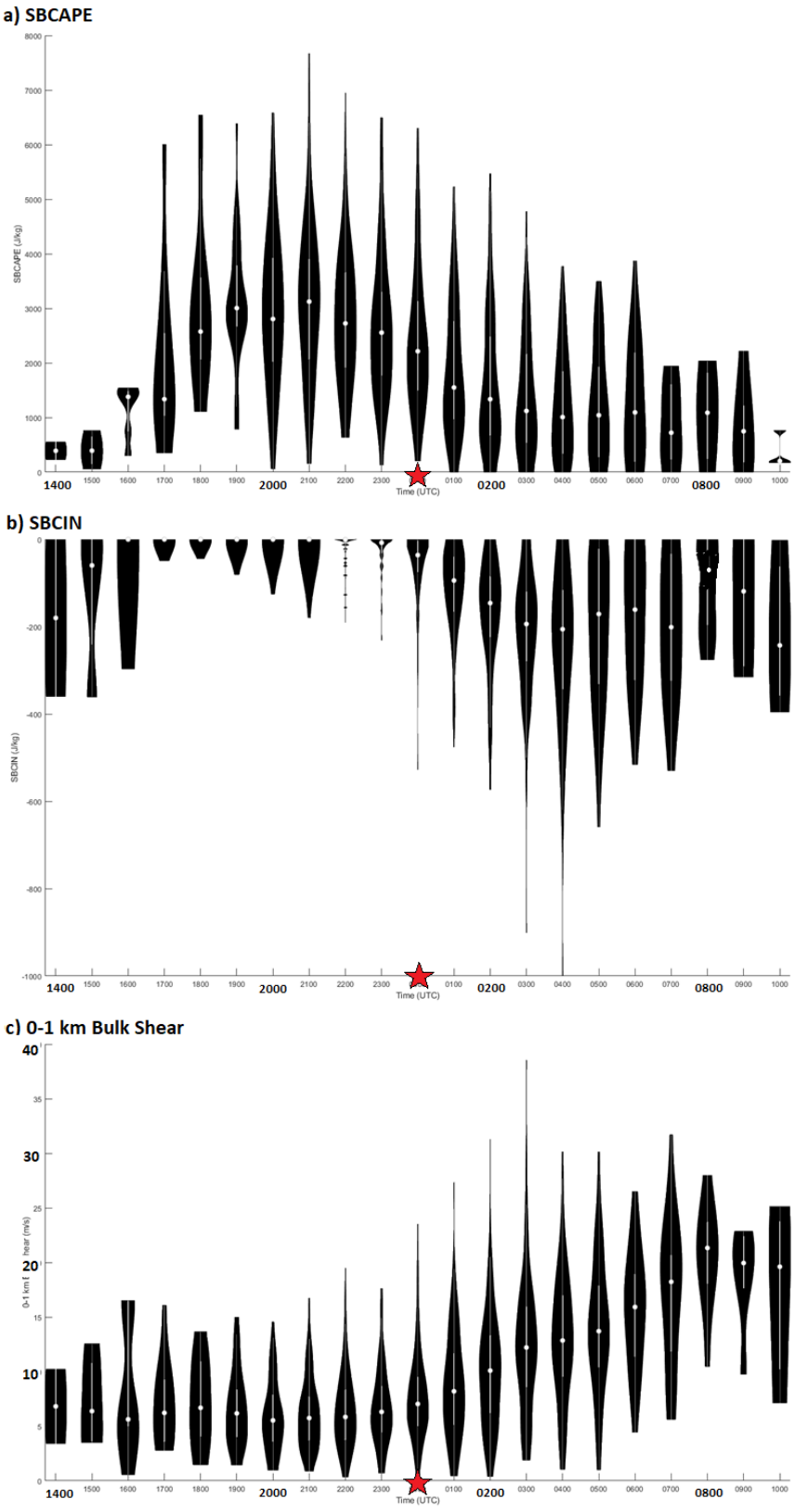

Figure 6: Hourly distributions of surface-based a) CAPE, b) surface-based CIN, and c) 0-1 km bulk shear. Each hour displays a violin plot containing the kernel density estimation of the distribution. The thin white line represents the interquartile range, and the white dot represents the median.

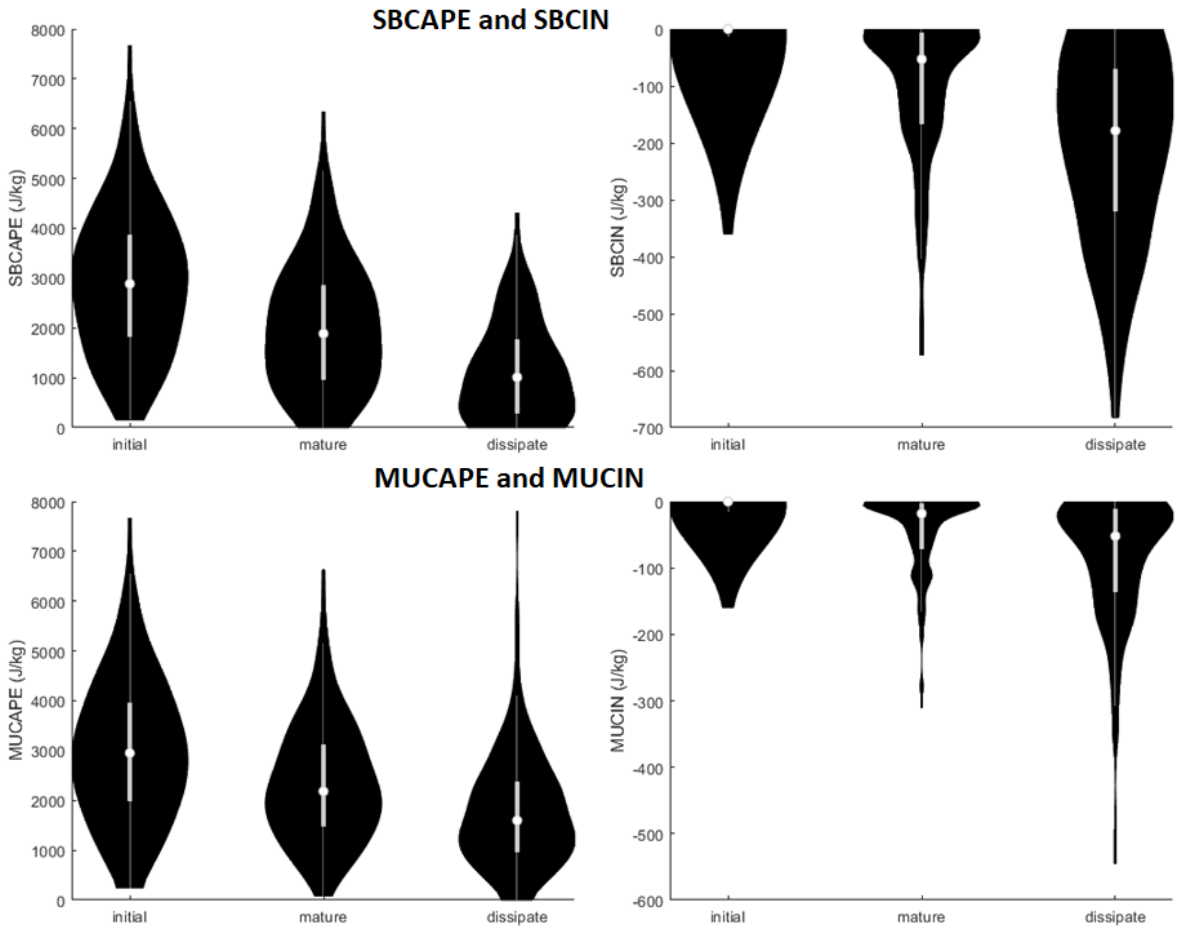

Figure 7: As in Fig. 6, but for distributions of surface-based CAPE and CIN (top) and most-unstable CAPE and CIN (bottom), binned with respect to the maturity of the supercell.

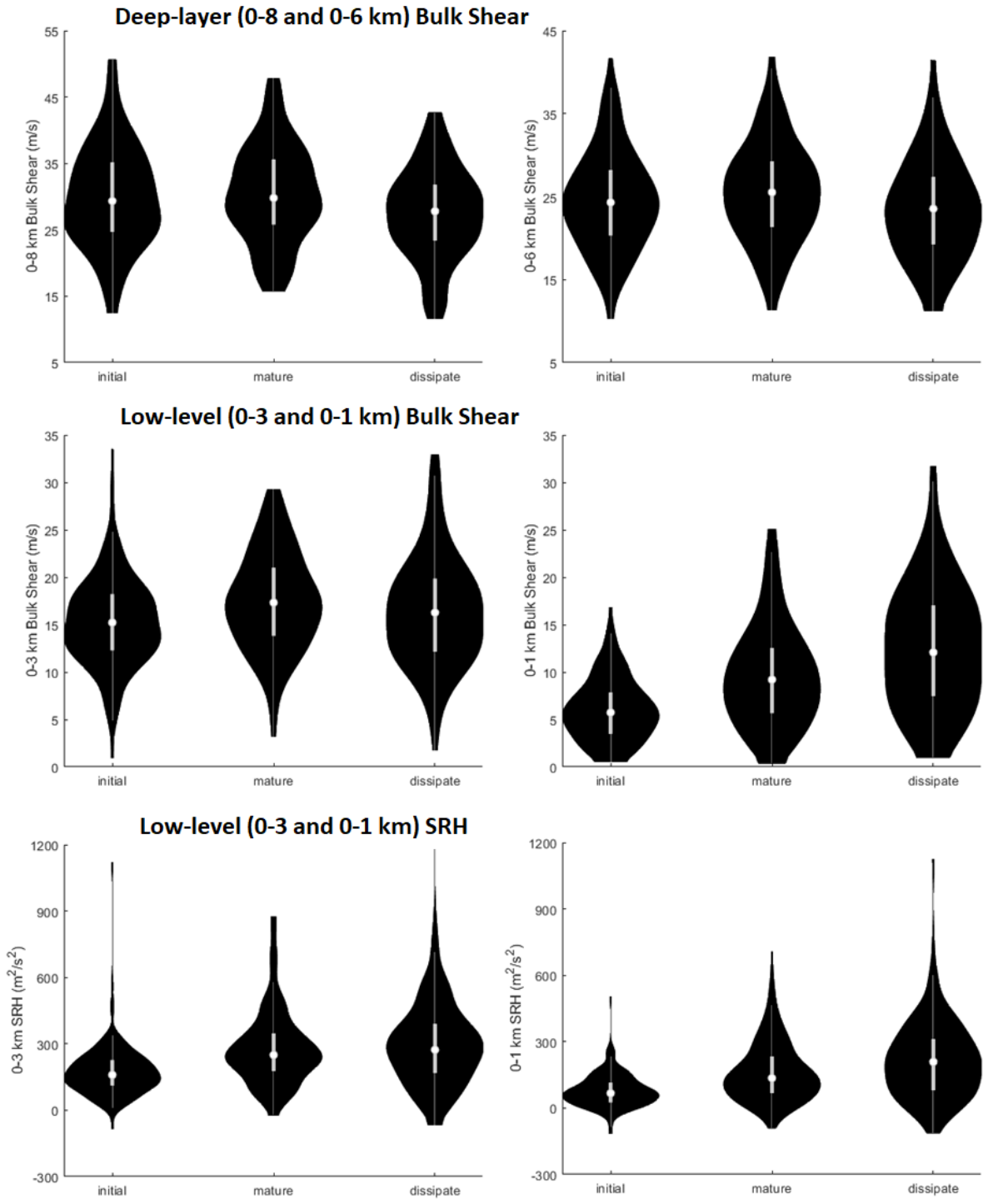

Figure 8: As in Fig. 7, but for distributions of deep-layer bulk shear (top), low-level bulk shear (middle), and low-level SRH (bottom).